IEEE Photonics Journal
An IEEE Photonics Society Publication

Open Access

Ultra High *Q* and Widely Tunable Mie Resonance Nanofilter at Telecom Wavelengths

Volume 13, Number 3, June 2021

Danyang Yao
Yong Zhang
Yan Huang
Yan Liu
Genquan Han, *Member, IEEE*
Yue Hao, *Senior Member, IEEE*

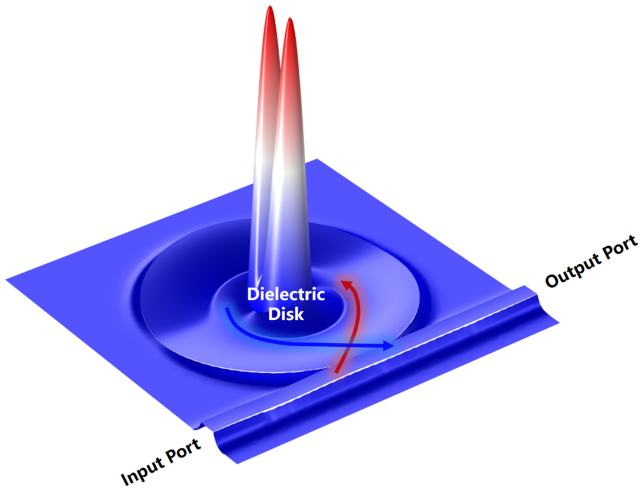

DOI: 10.1109/JPHOT.2021.3087743

Ultra High *Q* and Widely Tunable Mie Resonance Nanofilter at Telecom Wavelengths

Danyang Yao, Yong Zhang, Yan Huang, Yan Liu, Genquan Han, *Member, IEEE*, and Yue Hao, *Senior Member, IEEE*

Wide Bandgap Semiconductor Technology Disciplines State Key Laboratory, School of Microelectronics, Xidian University, Xi'an 710071, China

DOI:10.1109/JPHOT.2021.3087743
This work is licensed under a Creative Commons Attribution 4.0 License. For more information, see https://creativecommons.org/licenses/by/4.0/

Manuscript received May 29, 2021; accepted June 5, 2021. Date of publication June 9, 2021; date of current version June 30, 2021. This work was supported in part by the National Key Research and Development Project under Grants 2018YFB2200500, 2018YFB2202800, and in part by National Natural Science Foundation of China under Grants 62004145, 62025402, 62090033, 91964202, 92064003, 61874081, 61851406, and 62004149 Corresponding author: Yan Liu (e-mail: xdliuyan@xidian.edu.cn).

Abstract: Mie resonators offer a novel way for the subwavelength localization of light, showing large local field enhancement without metal optical absorption. In this paper, an ultra-high quality factor *Q* and widely tunable Mie resonance nanofilter at telecom wavelengths is presented. The loss mechanisms in this hybrid resonators are systematically analyzed. A selected high-index Ge disk embedded at the center of plasmonic nanocavity acts well as a Mie resonator for coupling the incident light. Based on the theoretical analysis and modeling, a widely tunable spectra linewidth from 14.2 *nm* to 1.2 *nm* and the maximum corresponding *Q* as high as 1292 is achieved. The Mie resonance nanofilters provide the possibility to make high performance and practical resonance component for nanophotonics integration.

Index Terms: Coupled resonators, optical filters, photonic integrated circuits, surface plasmon polaritons, wavelength filtering devices.

1. Introduction

Future telecommunications and optical logic applications will need a high integration level of photonic circuits to bridge the enormous gap compared with electronics circuits [1]. Due to limited refractive index contrast, the traditional dielectric optical devices or circuits have difficulty to decrease the footprint into nanoscale [2]. Plasmonic optics, which uses the strong confinement properties of surface plasmon polaritons (SPP) trapped on the surface of metals, can be utilized to guide light in volumes far beyond the diffraction limit, offering a potential method to merge photonics and electronics together with the equivalent scale integration level [3]–[5].

As one of the most important devices in optical communication field, plasmonic filters have been widely studied, such as tooth-shaped waveguide [6], [7], plasmonic grating [8]–[10], ring [11] and nanodisk resonators filter [12], [13]. All these structures show not only high bandpass or bandstop filtering performance, but also nanoscale size. In a modern optical communication system, in particular, the dense wavelength division multiplexing (DWDM) technology, requiring a large number of selected channels to enhance capacity of optical communication, which means optical filters with narrowband and multichannels performance are urgent needed [14]. Whereas,

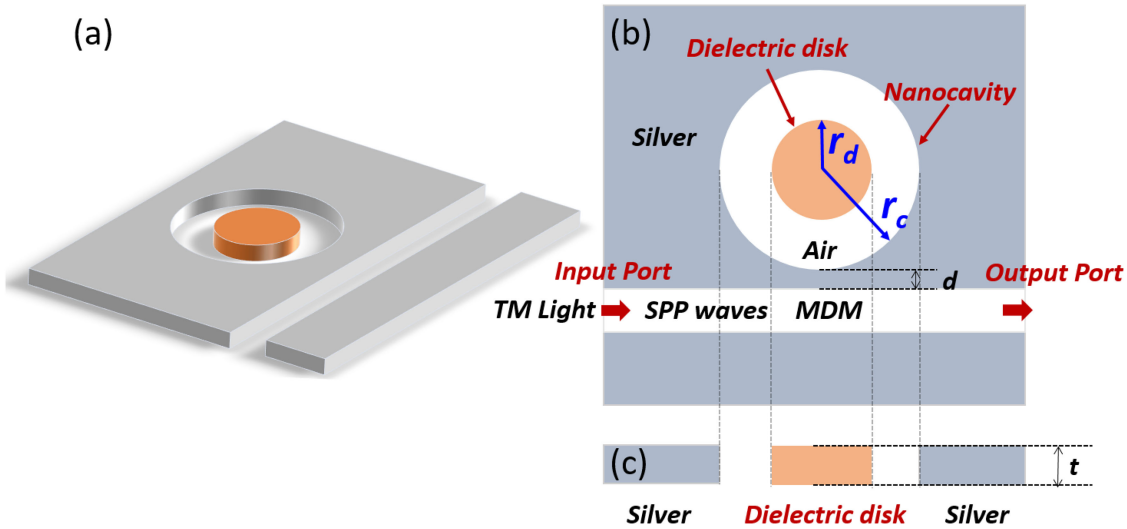

Fig. 1. (a) The 3D schematic of the Mie resonance nanofilter structure with an MDM slot waveguide. (b) The schematic of horizontal cross section. (c) The schematic of vertial cross section.

for those filters based on SPP principle, metals such as gold or silver involve inevitable absorption losses, which seriously affect the devices performance and hinder the practical applications. The latest reports on plasmonic filters do suggest that it is hard to reduce the transmission spectra linewidth below 20 *nm* [15]–[17]. In contrast, Mie resonators offer a novel way for the subwavelength localization of light, showing large local field enhancement in the high refractive index material [18]–[20]. Based on the Mie theory [21], the radius *r* of a particle plays a key role to arouse the Mie resonance when it becomes comparable to the wavelength inside the particle. As the advantages of Mie type resonators become more and more clear, those novel optical components have already shown remarkable optical effects and applications, including low loss meta-optics [22], [23], resonator [24], [25], spatial light absorption and filtering [26]–[30], beam control [31]–[33], slow light modulation [34]. Recently, optical energy transmission in subwavelength waveguides were achieved by resonant dielectric nanoparticle chains, representing an alternative method to plasmonic waveguide [35], [36]. Since plasmonic photonics encounter the performance bottleneck on the road to mature, it is worth considering to develop complementary and even alternative technology such as Mie resonance for large scale photonic integration, system miniaturization and novel devices.

In this paper, we propose a Mie resonance nanofilter structure. A selected high-index Ge disk is purposely embedded at the center of the plasmonic nanocavity, acting as a low loss resonator for coupling the incident light. The tuning and loss mechanisms of this hybrid resonators are investigated theoretically. Under finite element method (FEM) simulation environment, the resonance wavelengths and *Q* factors are tuned continuously by the geometry parameters, according well with the numerical predictions. Through optimization, the linewidth of filters can be widely tuned from 14.2 *nm* to 1.2 *nm*, and the maximum *Q* factor is obtained as high as 1292. These Mie resonance nanofilters represent a novel way to make high performance and practical plasmonic resonance optics, and further bridge the process gap with electronics circuits.

2. Structure Design and Theory Analysis

The proposed nanofilter structure is depicted in Fig. 1. This design consists of a plasmonic nanocavity with a high-index dielectric disk centrally embedded and a straight metal dielectric metal (MDM) slot waveguide that serves as an evanescent wave coupler. *d* is the gap between

the nanocavity and the MDM waveguide, r_c and r_d is the radius of nanocavity and dielectric disk respectively, and t is the thickness of the dielectric disk. The materials in gray and white are silver and air, and the dielectric disk is highlighted in orange. Referring to fig. 1(b), the working principle of the proposed filter is that the SPP waves is firstly excited at the input port by the transverse magnetic (TM) polarized light, then it propagates along the MDM waveguide and couples into the resonator with specific wavelength. This behavior could be described as an optical filter.

According to the temporal coupled-mode theory [37] when the SPPs waves propagate in the MDM waveguide, the energy can be coupled into the nanocavity resonator. Due to the weak coupling between the two degenerate modes for this symmetric structure [38], only single nanocavity transmission spectrum will exhibit a dip at the resonance wavelength. In principle, this proposed nanocavity resonator couples two main resonance modes named SPP mode and Mie mode. The resonance wavelength of SPP modes λ_{SPP} changes in direct proportion to the effective refraction index of resonator n_{eff} and the radius of plasmonic cavity r_c [39]. In contrast to SPP resonance mode, Mie mode attracts nearly all the electromagnetic field into the high-index dielectric disk [19]. Consequently, its resonance properties have close association with the disk. According to the Mie theory, the resonance occurs when the wavelength inside the particle is approximately equal to the diameter of the disk, and shows an enhanced electromagnetic field of the corresponding harmonic both inside and outside of the particle. The resonance condition of Mie resonance can be defined as [21],

$$m\lambda_{Mie}/n_d = 2r_d \tag{1}$$

where m are the resonance mode numbers of Mie mode, λ_{Mie} is the wavelength in vacuum, n_d and r_d is the refractive index and radius of the dielectric disk respectively.

Q factor, as another important parameter of nanofilters, measuring the energy leakage rate of the mode confined inside an optical cavity, can be expressed as the summation of two main depletion mechanisms [40], [41].

$$1/Q_{total}=1/Q_{abs}+1/Q_{esc} \tag{2}$$

where Q_{total} is total quality factor of this resonator, and Q_{abs} and Q_{esc} denotes the quality factors accounting for the material absorption loss and energy escaping loss, respectively.

Besides, the transmission intensity distribution near the resonance wavelength follows the Lorentizan lineshape, therefore, the Q factor could be approximately expressed in another form $Q_{total}\approx\lambda_0/\lambda_{FWHM}$ [41], where λ_0 is the resonance wavelength, and λ_{FWHM} is the linewidth of the transmission peak (full width at half maximum, FWHM). That means the Q factor also represents the accuracy of wavelength selectivity [42]. For filter applications, one can consider that the larger the Q factor, the more channels could be arranged within a limited spectral band.

The material loss related Q_{abs} will be first investigated. As shown in fig. 2(a), in a traditional nanocavity resonator, the coupled optical energy is individually dissipated in the plasmonic cavity as the form of SPPs wave. While for the proposed hybrid nanocavity resonator design, not only the plasmonic metallic cavity but also the dielectric disk will both absorb the coupled light. As shown in fig. 2(b), majority of the coupled optical energy transforms as SPPs wave along the metallic cavity surface, and only a small amount of energy leaks to the dielectric disk. Oppositely, as shown in fig. 2(c), Mie mode couples almost all the energy into the low loss dielectric disk, yet a tiny amount of energy inevitably leaks to the cavity and is unavoidably absorbed. So the total absorption decay rate $1/Q_{abs}$ for this hybrid Mie mode should take account of decay rates both in a dielectric disk $1/Q_{abs(d)}$ and cavity $1/Q_{abs(c)}$, can be written as [43],

$$1/Q_{abs}=1/Q_{abs(d)}+1/Q_{abs(c)}= 2f_d\frac{n_{i(d)}}{n_{r(d)}} + f_c\frac{\alpha_c}{k} \tag{3}$$

where f_d and f_c are the filling factor of coupled field energy in dielectric disk and plasmonic cavity, defined as the ratio between the electromagnetic field energy in the loss materials and the total energy in the resonator, $n_{i(d)}$ and $n_{r(d)}$ is the imaginary and real part of the refractive index of a dielectric disk, α_c is the absorption coefficient of the cavity, and k is the wave vector. Therefore, for

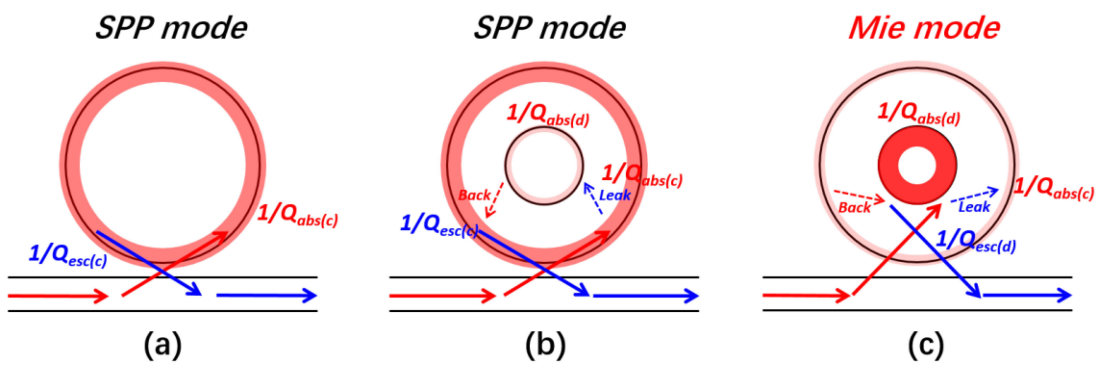

Fig. 2. Illustration of loss mechanism in traditional nanocavity and Mie resonance nanocavity. (a) Losses of SPP mode in traditional nanocavity. (b) and (c) Losses of SPP mode and Mie mode in Mie resonance nanocavity.

a hybrid resonator with two absorptive regions, the absorption decay rate depends on the energy filling factor and the absorption coefficient of each region.

Next, the escaping loss related Q_{esc} will be analyzed. As shown in fig. 2(c), unlike the absorption losses occur inside the dielectric disk and metallic cavity in parallel, the escaping losses of Mie mode is a scattering of light caused by a nano-sized particle, which have the main channel from the scatterer to DMD waveguide for dissipation. So the final escaping decay rate Q_{esc} depends on energy filling factor and scattering loss of dielectric disk, can be expressed as [44],

$$1/Q_{esc} = 1/Q_{esc(d)} = f_d \omega^{-1} \gamma_{esc(d)} \tag{4}$$

where ω is the frequency, the escaping loss $\gamma_{esc(d)}$ donates the energy scattering loss by the dielectric disk, which is given by $\gamma_{esc(d)} = N\sigma c/n_{r(d)}$ [44], where N is number density, σ is the horizontal cross section of dielectric disk and c is the speed of light. Inserting the equation (3) and equation (4) into the equation (2), the total quality factor Q_{total} can be further written as,

$$1/Q_{total} = f_d \left(\frac{2n_{i(d)} + \omega^{-1} N\sigma c}{n_{r(d)}} \right) + f_c \frac{\alpha_c}{k} \tag{5}$$

In this hybrid cavity case, assuming the cavity loss α_c/k is constant and the geometric dimensions of resonator remain unchanged, the Q_{total} is directly limited by the refractive index of dielectric disk. In general, a high real part of a dielectric material index, on the one hand, is both beneficial to alleviating the absorption loss and escaping loss. And on the other hand, it makes more energy confined in the disk, which means the value of f_d will get closer to 1, and dramatically influence on the decrease of f_c. This results may be intuitively understood as the result of alleviated scattering for nanoparticles with a large refractive index contrast between particles and surrounding [45]. In addition, based on the analysis and according to the equation (5), if the imaginary part of index dielectric material $n_{i(d)}$ increases to the value comparable to the escaping loss $\omega^{-1}N\sigma c$, the absorption of the dielectric material will no longer be ignored for Q_{total} evaluation.

In conclusion, high-index and low loss dielectric materials are the desirable choices for Mie resonance resonators applications. In the near-IR spectral ranges, unfortunately, the availability of high-index materials with low material losses is scarce, leaving GaAs, Si and Ge as the few high-index dielectric material candidates to be investigated for high performance Mie resonance nanofilters. In what follows, it is shown how the material properties and geometries affect the performance of Mie resonance filters. Need to noted that 2D FEM simulation method is used and the thickness of the disk is thought to be infinite size ($t \sim \infty$) without reflection in vertical direction. Meanwhile, for the materials modeling, the well-known Lorentz-Drude model is used for silver, and this fit provides an accurate description of the dielectric data in the wavelength range of

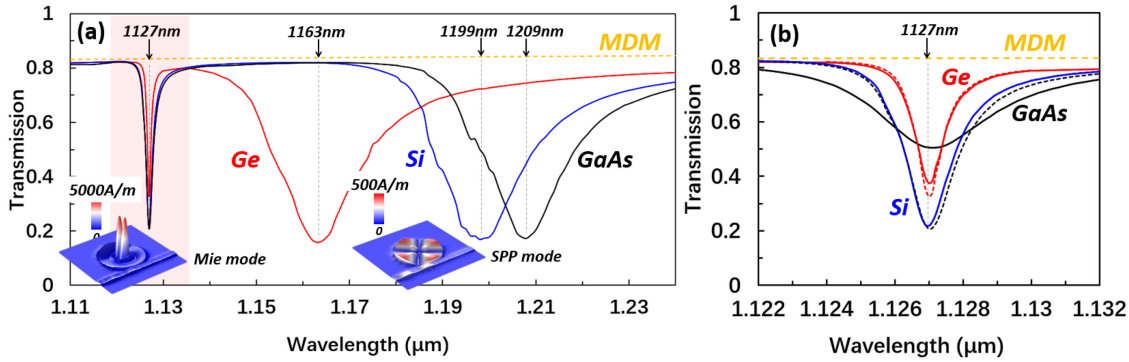

Fig. 3. (a) Transmission spectra of Mie resonance nanofilter with GaAs (black), Si (blue) and Ge (red) dielectric disk embedded, and transmission spectra of pure MDM (yellow) waveguide. left inset: 3D magnetic field intensity distribution of Mie mode. And right inset: SPP mode. (b) A transmission spectra comparison near the Mie mode resonance wavelength between loss less (dotted line) and loss (solid line) materials.

1000-2000 *nm* [46]. In addition, the refractive index data of semiconductor GaAs, Si and Ge could be found in Ref. [47], [48].

3. Material Evaluation and Selection

Fig. 3(a) shows the transmission spectra (1.1 to 1.24 μm) of nanofilters with loss less GaAs ($n_{r(d)} = 3.35$), Si ($n_{r(d)} = 3.47$) and Ge ($n_{r(d)} = 4.21$) dielectric disk. In order to identify different mode, Mie and SPP resonance modes are labeled as Mie mode$_{\mathrm{mn}}$ and SPP mode$_{\mathrm{mn}}$ respectively, where m is the radial number of field maxima along the radius and n is the azimuthal number of magnetic dipoles across the inner circumference of the disk. The GaAs based nanofilter with geometry parameters $d = 10$ *nm*, $r_c = 500$ *nm*, and $r_d = 200$ *nm* exhibits Mie mode$_{11}$ resonance at the wavelength of 1127 *nm*. Further, the high-index materials Si and Ge are performed. In order to make comparison for Mie mode at the same wavelength, the Si and Ge based nanofilters decrease r_d to 193 *nm* and 159 *nm* for tuning the resonance wavelength to the same value as GaAs. In contrast to SPP resonance mode shown in the right bottom inset picture, the electromagnetic field of Mie mode is nearly all confined inside the high-index disk and the maximum magnetic intensity is one order magnitude higher than SPP mode. Consequently, the interaction between light and matter is sensitive to the optics and geometry parameters of the dielectric disk. Moreover, as shown in fig. 3(b), the imaginary parts of index are added to investigate the filtering performance differences between loss less and loss materials. Since the GaAs ($n_{i(d)} = 3.9\times10^{-3}$) have a relatively high absorption coefficient, its degradation in linewidth is more remarkable than the other two materials, Si ($n_{i(d)} = 1\times10^{-13}$) and Ge ($n_{i(d)} = 2.7\times10^{-4}$).

Fig. 4 makes the further analysis that tries to reveal the deep connections between Q factors and material refractive index. The curves are retrieved from the corresponding transmission spectra and mode field intensity distributions. First the Q_{total} is calculated by the ratio between wavelength and linewidth fitted by Lorenz curve. As the reference noted [37], the value of a resonance dip in a transmission spectrum could be expressed as $[1/Q_{abs}/(1/Q_{abs}+ 1/Q_{esc})]^2$, and combined with the equation (2), the Q_{abs} and Q_{esc} can be solved at the same time. Focusing on the red dotted curve, as the real part of the refractive index of the disk increases, the energy filling factor of the plasmonic cavity (as shown in the right first picture of fig. 4) drops dramatically, indicating suppressed energy leakage out of the dielectric disk and lowered absorption loss in plasmonic cavity. Expectedly, Ge based nanofilter shows the highest Q_{total} value of 1199 compared with GaAs of 648 and Si of 696. The Q_{abs} and Q_{esc} calculated curves show the same tendency when the high-index dielectric materials are used. The blue dotted curve shows the further analysis that how the imaginary parts

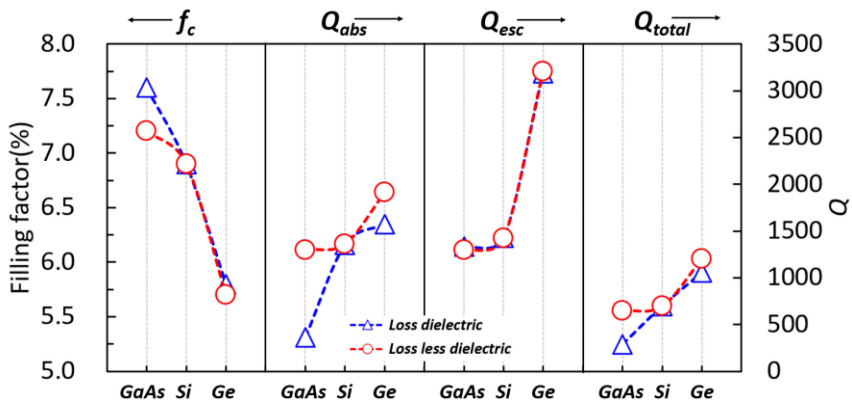

Fig. 4. The calculated filling factors f_c and Q factors for nanofilters with GaAs, Si and Ge loss and loss less materials.

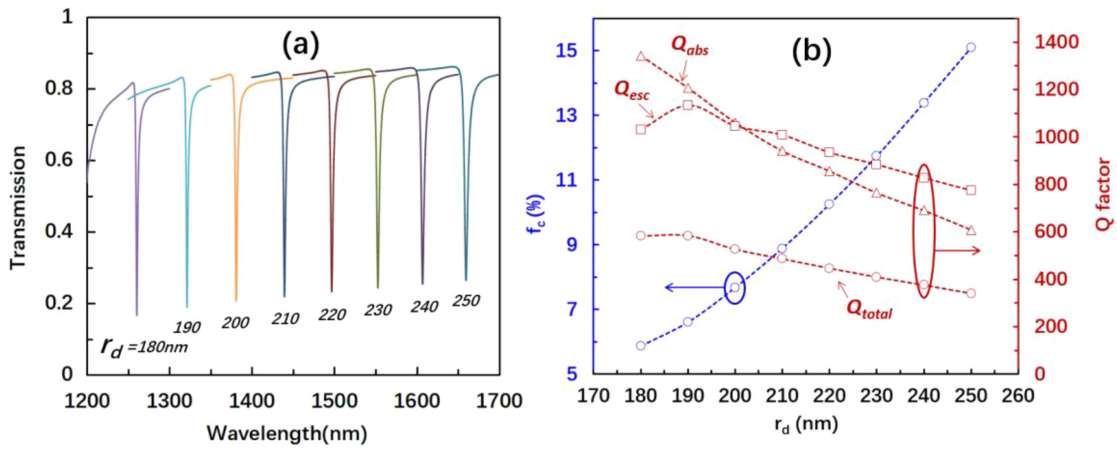

Fig. 5. (a) Transmission spectra tuned by the radius of Ge disk r_d. (b) Blue curve shows the resonance wavelength as a function of r_d. Red curve shows the Q_{total} factor as a function of r_d.

of index affects the Q factor. After the material losses are considered, the deterioration of Q_{total} is mainly due to the drop of Qabs as predicted by equation (3). Though Ge have a higher absorption coefficient than Si, the Q_{total} of Ge disk is as high as 1153, which is still much higher than 696 of Si disk. Since Ge owns high refractive index and moderate absorption coefficient, it shows an enormous potential to acts as a high performance Mie resonance component at near-infrared range. In addition, the fast development of Germanium-on-insulator(GeOI) substrate provides an attractive platform for Ge based photonics devices integration [49]. Based on the analysis above, Ge is the best material for Mie mode coupling among those three candidate materials.

4. Structure Optimization and Discussion

In this section, the selected Ge based nanofilter will be performed by structure optimization. The geometry parameters $d = 10$ *nm*, $r_c = 500$ *nm* is fixed. As shown in fig. 5(a), when r_d increases from 180 *nm* to 250 *nm* with a step of 10 *nm*, a near-linear resonance wavelength redshift from 1260.6 *nm* to 1660.0 *nm* with a fitted tuning rate of 5.7 *nm/nm* is observed. The wavelength tuning results tallies well with the Mie mode resonance condition included in equation (1). The parameter

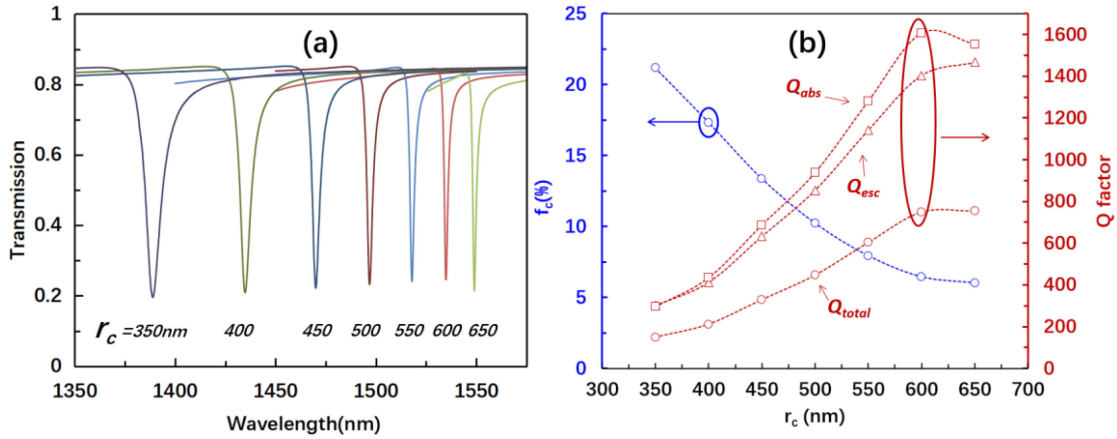

Fig. 6. (a) Transmission spectra tuned by the radius of nanocavity r_c. (b) Blue curve shows the resonance wavelength as a function of r_c. Red curve shows the Q_{total} factor as a function of r_c.

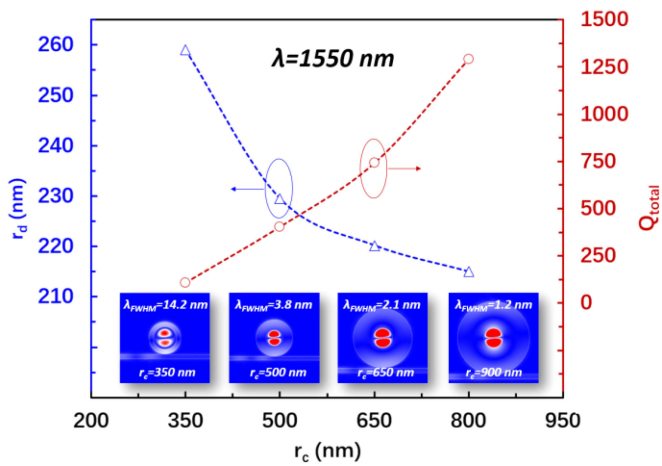

Fig. 7. Widely tunable nanofilter designs working at telecom wavelength.

λ_{FWHM} is extracted from the Lorentz fitted transmission peak, broadening from 2.16 *nm* to 4.86 *nm*. Fig. 5(b) shows that the corresponding Q_{total} factor is found to drop from 583 to 341, and the calculated Q_{abs} and Q_{esc} follows the same downward trend as the filling factor f_c rapidly increases. This phenomenon can be explained that the enhanced scattering leads to an aggravated cavity absorption loss, when the dielectric disk size increases.

The tuning properties by the radius of nanocavity r_c are also investigated. Geometry parameters are fixed as $d = 10$ *nm*, $r_d = 220$ *nm*. As shown in fig. 6(a), when the radius of nanocavity r_c increases from 350 *nm* to 650 *nm* with a step of 50 *nm*, an expected redshift of resonance wavelength is observed. The wavelength peak starts at 1389.6 *nm* with a trends towards saturation near at 1549.2 *nm* with an average tuning rate of 0.5 *nm/nm*. Meanwhile, the λ_{FWHM} shows the reverse trend and dramatic improves from 9.30 *nm* to 2.05 *nm* with Q_{total} factor increasing from 149 to 755 correspondingly. The downtrend of f_c indicates an enhancement of optical field with less energy escaping from the Ge disk, which is both beneficial to the Q_{abs} and Q_{esc} improvement.

Based on the numerical analysis above, an effective design rules towards tunable filters could be concluded, that the radius of dielectric disk r_d is a more efficient role for shifting the filtering wavelength, and the radius of nanocavity r_c is a trade-off parameter to make a balance between high Q factor and small device size. Fig. 7 shows the widely tunable characteristic at telecom

wavelength. When small $r_c = 350$ *nm* and proper $r_d = 259$ *nm* is used, the nanofilter shows a wide filtering performance with $\lambda_{FWHM} = 14.2$ *nm* (corresponding $Q_{total} = 109$) near the resonance wavelength of 1550 *nm*. The linewidth can be readily narrowed by increasing the radius of cavity. The maximum r_c reaches no more than 800 *nm* in case of introducing high order SPP modes into C band (1530-1565 *nm*). Finally, the linewidth is narrowed to 1.2 *nm* (corresponding $Q_{total} = 1292$) when $r_c = 800$ *nm* and $r_d = 215$ *nm*. The displayed tunable characteristics of this kind of nanofilters can support single to maximum 30 channels in optical filtering applications.

5. Conclusion

In summary, an ultra-high Q and widely tunable Mie resonance nanofilter at telecom wavelengths is proposed. The tuning and loss mechanism is theoretically explained. In the near-infrared range, Ge material disk is verified to act well as a high-index and low loss Mie resonator for coupling the incident light. Through optimization, the linewidth of filters can be widely tuned from 14.2 *nm* to 1.2 *nm*, the maximum Q factor is obtained as high as 1292. This Mie resonance nanofilter shows a promising perspective to make high performance and practical plasmonic resonance optics, and further bridge the process gap with electronics circuits.

References

[1] Yariv and P. Yeh, *Photonics: Optical Electronics in Modern Communications*, 6th ed. Oxford Univ. Press, 2006.
[2] Y. Vlasov and S. Mcnab, "Losses in single-mode silicon-on-insulator strip waveguides and bends," *Opt. Exp.*, vol. 12, pp. 1122–1131, 2004.
[3] W. L. Barnes, A. Dereux, and T. W. Ebbesen, "Surface plasmon subwavelength optics," *Nature*, vol. 424, pp. 824–830, 2003.
[4] G. Veronis and S. Fan, "Bends and splitters in metal-dielectric-metal subwavelength plasmonic waveguides," *Appl. Phys. Lett.*, vol. 87, 2005, Art. no. 131102.
[5] S. I. Bozhevolnyi, V. S. Volkov, E. Devaux, J. Y. Laluet, and T. W. Ebbesen, "Channel plasmon subwavelength waveguide components including interferometers and ring resonators," *Nature*, vol. 440, pp. 508–511, 2006.
[6] X. S. Lin and X. G. Huang, "Tooth-shaped plasmonic waveguide filters with nanometeric sizes," *Opt. Lett.*, vol. 33, pp. 2874–2876, 2009.
[7] F. Hu and H. Yi, and Z. Zhou, "Wavelength demultiplexing structure based on arrayed plasmonic slot cavities," *Opt. Lett.*, vol. 36, pp. 1500–1502, 2011.
[8] B. Wang and G. P. Wang, "Plasmon Bragg reflectors and nanocavities on flat metallic surfaces," *Appl. Phys. Lett.*, vol. 87, 2005, Art. no. 013107.
[9] Z. Han, E. Forsberg, and S. He, "Surface plasmon Bragg gratings formed in metal-insulator-metal waveguides," *IEEE Photonic. Tech. L.*, vol. 19, no. 2, pp. 91–93, Jan. 2007.
[10] P. Neutens, L. Lagae, G. Borghs, and P. Van Dorpe, "Plasmon filters and resonators in metal-insulator-metal waveguides," *Opt. Exp.*, vol. 20, pp. 3408–3423, 2012.
[11] X. Wang, P. Wang, C. Chen, J. Chen, and Q. Zhan,"Plasmonic racetrack resonator with high extinction ratio under critical coupling condition," *J. Appl. Phys.*, vol. 107, 2010, Art. no. 124517.
[12] F. Lu, Z. Wang, K. Li, and A. Xu, "A plasmonic triple-wavelength demultiplexing structure based on a MIM waveguide with side-coupled nanodisk cavities," *IEEE Trans. Nanotechnol.*, vol. 12, no. 6, pp. 1185–1190, Nov. 2013.
[13] Y. Liu, J. Yan, and G. Han,"The transmission characteristic of metal–dielectric–metal slot waveguide-based nanodisk cavity with gain medium," *IEEE Photon. J.*, vol. 7, no. 2, Apr. 2015, Art. no. 4500608.
[14] B. Mukherjee, "WDM optical communication networks: Progress and challenges," *IEEE J. Sel. Area. Commun.*, vol. 18, no. 10, pp. 1810–1824, Oct. 2000.
[15] A. Dolatabady and N. Granpayeh,"All-optical logic gates in plasmonic metal–insulator–metal nanowaveguide with slot cavity resonator," *J. Nanophoton.*, vol. 11, 2017, Art. no. 026001.
[16] S. Khani, M. Danaie, and P. Rezaei, "Realization of single-mode plasmonic bandpass filters using improved nanodisk resonators," *Opt. Commun.*, vol. 420, pp. 147–156, 2018.
[17] Y. Qi *et al.*, "Theoretical study of a multichannel plasmonic waveguide notch filter with double-sided nanodisk and two slot cavities," *Results Phys.*, vol. 14, 2019, Art. no. 102506.
[18] A. I. Kuznetsov, A. E. Miroshnichenko, M. L. Brongersma, Y. S. Kivshar, and B. Luk'Yanchuk, "Optically resonant dielectric nanostructures," *Science*, vol. 354, 2016, Art. no. 2472.
[19] Y. Kivshar and A. Miroshnichenko, "Meta-optics with Mie resonances," *Opt. Photon. News*, vol. 28, pp. 24–31, 2017.
[20] M. V. Rybin *et al.*, "High-Q supercavity modes in subwavelength dielectric resonators," *Phys. Rev. Lett.*, vol. 119, 2017, Art. no. 243901.
[21] C. F. Bohren and D. R. Huffman, *Absorption and Scattering of Light by Small Particles*. Hoboken, NJ, USA: Wiley, 1983.
[22] K. Koshelev, A. Bogdanov, and Y. Kivshar, "Meta-optics and bound states in the continuum," *Sci. Bull*, vol. 64, pp. 836–842, 2019.

[23] T. Liu, R. Xu, P. Yu, Z. Wang, and J. Takahara, "Multipole and multimode engineering in Mie resonance-based metastructures," *Nanophotonics*, vol. 9, pp. 1115–1137, 2020.
[24] M. Garín, R. Fenollosa, R. Alcubilla, L. Shi, L. F. Marsal, and F. Meseguer, "All-silicon spherical-Mie-resonator photodiode with spectral response in the infrared region," *Nat. Commun.*, vol. 5, 2014, Art. no. 3440.
[25] X. Zambrana-Puyalto, and N. Bonod, "Purcell factor of spherical Mie resonators," *Phys. Rev. B*, vol. 91, 2015, Art. no. 195422.
[26] F. J. Bezares *et al.*, "Mie resonance-enhanced light absorption in periodic silicon nanopillar arrays," *Opt. Exp.*, vol. 21, pp. 27587–27601, 2013.
[27] Z. Wang *et al.*, "Broadband optical absorption by tunable Mie resonances in silicon nanocone arrays," *Sci. Rep.*, vol. 5, pp. 1–6, 2015.
[28] F. Shen, Q. Kang, J. Wang, K. Guo, Q. Zhou, and Z. Guo, "Dielectric metasurface-based high-efficiency mid-infrared optical filter," *Nanomaterials*, vol. 8, 2018, Art. no. 938.
[29] R. C. Ng, J. C. Garcia, J. R. Greer, and K. T. Fountaine, "Polarization-independent, narrowband, near-IR spectral filters via guided mode resonances in ultrathin a-Si nanopillar arrays," *ACS Photon.*, vol. 6, pp. 265–271, 2019.
[30] A. D. Utyushev *et al.*, "Engineering novel tunable optical high-Q nanoparticle array filters for a wide range of wavelengths," *Opt. Exp.*, vol. 28, pp. 1426–1438, 2020.
[31] L. Holsteen, S. Raza, P. Fan, P. G. Kik, and M. L. Brongersma, "Purcell effect for active tuning of light scattering from semiconductor optical antennas," *Science*, vol. 358, pp. 1407–1410, 2017.
[32] Forouzmand and H. Mosallaei, "Dynamic beam control via Mie-resonance based phase-change metasurface: A theoretical investigation," *Opt. Exp.*, vol. 26, pp. 17948–17963, 2018.
[33] M. Shaltout, V. M. Shalaev, and M. L. Brongersma, "Spatiotemporal light control with active metasurfaces," *Science*, vol. 364, pp. 1–10, 2019.
[34] R. Søren, "Slow light using magnetic and electric Mie resonances," *Opt. Lett.*, vol. 45, pp. 1260–1263, 2020.
[35] R. S. Savelev, A. P. Slobozhanyuk, A. E. Miroshnichenko, Y. S. Kivshar, and P. A. Belov, "Subwavelength waveguides composed of dielectric nanoparticles," *Phys. Rev. B*, vol. 8, 2014, Art. no. 035435.
[36] R. M. Bakker, Y. F. Yu, R. Paniagua-Dominguez, B. Luk'yanchuk, and A. I. Kuznetsov, "Resonant light guiding along a chain of silicon nanoparticles," *Nano Lett.*, vol. 17, pp. 3458–3464, 2017.
[37] Q. Li, T. Wang, Y. Su, M. Yan, and M. Qiu, "Coupled mode theory analysis of mode-splitting in coupled cavity system," *Opt. Exp.*, vol. 18, 2010, Art. no. 8367.
[38] Z. Zhang, M. Dainese, L. Wosinski, and Q. Min, "Resonance-splitting and enhanced notch depth in SOI ring resonators with mutual mode coupling," *Opt. Exp.*, vol. 16, 2008, Art. no. 4621.
[39] Y.-Y. Xie, Y.-X. Huang, W.-L. Zhao, W.-H. Xu, and C. He, "A novel plasmonic sensor based on metal–insulator–metal waveguide with side-coupled hexagonal cavity," *IEEE Photon. J.*, vol. 7, no. 2, Apr. 2015, Art. no. 4800612.
[40] K. Vahala, *Optical Microcavities*. Singapore: World Scientific, 2004.
[41] X. Tu, S. L. Chen, C. Song, T. Huang, and L. J. Guo, "Ultrahigh q polymer microring resonators for biosensing applications," *IEEE Photon. J.,* vol. 11, no. 2, pp. 1–10, Apr. 2019.
[42] M. Soltani, S. Yegnanarayanan, and A. Adibi, "Ultra-high q planar silicon microdisk resonators for chip-scale silicon photonics," *Opt. Exp.*, vol. 15, pp. 4694–4704, 2007.
[43] T. Xu, M. S. Wheeler, H. E. Ruda, M. Mojahedi, and J. S. Aitchison, "The influence of material absorption on the quality factor of photonic crystal cavities," *Opt. Exp.*, vol. 17, pp. 8343–8348, 2009.
[44] T. J. Kippenberg, A. L. Tchebotareva, J. Kalkman, A. Polman, and K. J. Vahala, "Purcell-factor-enhanced scattering from si nanocrystals in an optical microcavity," *Phys. Rev. Lett.*, vol. 103, 2009, Art. no. 027406.
[45] G. Baranov *et al.*, "All-dielectric nanophotonics: The quest for better materials and fabrication techniques," *Optica*, vol. 4, pp. 814–825, 2017.
[46] D. Palik, *Handbook of Optical Constants of Solids*. Cambridge, MA, USA: Academic, 1998.
[47] T. F. Marple, "Refractive index of GaAs," *J. Appl. Phys.*, vol. 35, pp. 1241–1242, 1964.
[48] H. Li, "Refractive index of silicon and germanium and its wavelength and temperature derivatives," *J. Phys. Chem. Ref. Data*, vol. 9, pp. 561–658,1980.
[49] T. Akatsu *et al.*, "Germanium-on-insulator (GeOI) substrates—A novel engineered substrate for future high performance devices," *Mat. Sci. Semicon. Proc.*, vol. 9, pp. 444–448, 2006.